

## NUMERICAL INVESTIGATION OF CURVATURE AND TORSION EFFECTS ON WATER FLOW FIELD IN HELICAL RECTANGULAR CHANNELS

A. H. ELBATRAN<sup>1,4</sup>, O. B. YAAKOB<sup>1,2</sup>,  
Y. M. AHMED<sup>1,3,\*</sup>, H. M. SHABARA<sup>1,4</sup>

<sup>1</sup>Faculty of Mechanical Engineering, Universiti Teknologi Malaysia,  
81310, Skudai, Johor, Malaysia

<sup>2</sup>Marine Technology Center, Universiti Teknologi Malaysia,  
81310, Skudai, Johor, Malaysia

<sup>3</sup>Faculty of Engineering, Alexandria University, Alexandria, Egypt

<sup>4</sup>College of Engineering and Technology, Arab Academy for Science, Technology and  
Maritime Transport, Alexandria, Egypt

\*Corresponding Author: yasser@mail.fkm.utm.my

### Abstract

Helical channels have a wide range of applications in petroleum engineering, nuclear, heat exchanger, chemical, mineral and polymer industries. They are used in the separation processes for fluids of different densities. The centrifugal force, free surface and geometrical effects of the helical channel make the flow pattern more complicated; hence it is very difficult to perform physical experiment to predict channel performance. Computational Fluid Dynamics (CFD) can be suitable alternative for studying the flow pattern characteristics in helical channels. The different ranges of dimensional parameters, such as curvature and torsion, often cause various flow regimes in the helical channels. In this study, the effects of physical parameters such as curvature, torsion, Reynolds number, Froude number and Dean Number on the characteristics of the turbulent flow in helical rectangular channels have been investigated numerically, using a finite volume RANSE code Fluent of ANSYS workbench 10.1 UTM licensed. The physical parameters were reported for range of curvature ( $\delta$ ) of 0.16 to 0.51 and torsion ( $\lambda$ ) of 0.032 to 0.1. The numerical results of this study showed that the decrease in the channel curvature and the increase in the channel torsion numbers led to the increase of the flow velocity inside the channel and the change in the shape of water free surface at given Dean, Reynolds and Froude numbers.

Keywords: Helical rectangular channel, Torsion, Curvature, Free surface, Velocity.

<b>Nomenclatures</b>	
$A_c$	Flow cross sectional area, m <sup>2</sup>
DE	Dean Number
$D_h$	Hydraulic depth, m
Fr	Froude Number
$G_k$	Generation of turbulence kinetic energy
$G_\omega$	The generation of $\omega$ .
$h$	Depth of the channel, m
$h_h$	Hydraulic depth, m
$P$	Pitch, m
$P_w$	Wetted perimeter, m
$R$	Curvature radius, m
Re	Reynolds number
$U$	Mean channel water velocity, m/s
$u_i = (u \ v \ w)$	Velocity components in the directions of $x_i=(x \ y \ z)$
$W$	Width of channel, m
$Y_k$	The dissipation of k
$Y_\omega$	The dissipation of $\omega$
<i>Greek Symbols</i>	
$\delta$	Curvature
$\Gamma_k$	The effective diffusivity for k.
$\Gamma_\omega$	The effective diffusivity for $\omega$
$\lambda$	Torsion
$\mu$	Water Dynamic viscosity, N s/m <sup>2</sup>
$\rho$	Water density, kg/m <sup>3</sup>

## 1. Introduction

The fluid flow of velocity profile properties in straight pipe depends on the distance along the pipe, as the flow becomes fully developed. However, when the flow direction changes, i.e., through a curved pipe, the behaviour of the flow pattern of the fluid changed completely [1]. The flow is subjected to centrifugal forces from the curved wall to the center of the channel; which causes the highest velocity at the outside wall [2]. The interaction between centrifugal and viscous forces in the curved flow tends to certain characteristic motion, known as secondary flow [1].

The first attention for curved open channel flow pattern was noticed in 1876 and 1877 by Thomson [3, 4] who observed the curvature effects in the open channel flow. At the beginning of 20th century, Williams et al. [2] studied experimentally the effects of curvature on the flow field in curved pipe, and they noticed that because of the centrifugal effect, the maximum axial velocity was located at the outer wall of pipe.

Eustice [5] investigated experimentally the fluid flow field in curved pipe, but the scientific community was attracted to the flow in curved ducts instead, since the works of Dean for fluid flow in curved pipe [6] and curved channel [7] were carried out. Germano [8, 9] studied the effect of torsion helical pipe flow by using

the orthogonal coordinates system. Berger and Talbot [10] reviewed and discussed the developing and fully developed flows in curved and coiled pipes in steady and unsteady regimes. These studies were established to get more information about curved geometries in piping systems. Flow in helical pipe and the effect of curvature and torsion on the fluid flow have been studied by many researchers, especially in the fields of heat exchanger, steam generator, air conditioning systems, cooling pipes, aircraft intake, piping systems and biological systems [11]. In contrast, the flow in helical channels has been the subject of much lesser attention because of the flow is more complicated and it has lower applications. The flow in helical channel is a free surface flow, which varies from closed helical pipe.

The open helical channels have wide applications in nuclear, chemical, polymer processing, mining and mineral-processing industries. Also, they are used for heat and mass transfer applications. Authors in [12-15] investigated the flow in helical channels for particle spiral separators in the mineral-processing industries. They focused on determining the free surface shape, which depended on the geometrical parameters, especially torsion and flow rate. Researchers in [16-19] investigated and computed the helical flow in micro curved channel with micro mixing for various Dean Numbers, in which they concluded their study by improving and determining a new type of micromixers for chemical uses. Peerhossaini and Guer [20] studied the effect of curvature and torsion on the secondary flow vortices for sequence of curved channels with experiment; they proved that the vortex only was shifted under the effect of torsion.

Poskas et al. [21] and Simonis et al. [22] presented hydrodynamically and thermally the experimental and numerical investigations to increase the rate of heat transfer in rectangular cross-section helical channels, for laminar and turbulent flow. They focused on the heat transfer rate and hydraulic drag. In their research, they also made a comparison between helical and straight channels. For the helical channel modeling with rectangular cross section, authors in [23, 24] modeled numerically a fully developed free surface flow in a helical channel with finite pitch and rectangular section for laminar flow. They used finite volume method for their solutions and validated their results with experiment work. Furthermore, reference [25] also studied helical channel with turbulent flow and low Reynolds numerically.

From the above literatures, it is noticed that many researches had been conducted to investigate the flow characteristics in curved and helical pipes and channels, but it is important to recognize the hydraulic characteristics beforehand. Most of the previous studies were interested in the flow with low values of Reynolds and Dean Numbers.

In this research work, we studied the characteristics of the helical channel flow from the hydraulic point of view to expand the range of applications of the helical channels, especially in the field of renewable energy. As a result, this research focused on determining the velocity field pattern, velocity distribution, water velocity values, centrifugal force, the free surface interface and volume flow rate, with variations of geometrical parameters for turbulent water flow at high Reynolds, Dean and Froude Numbers.

## 2. Physical Model

The geometry of the problem is shown in Fig. 1, where  $R$  indicates the curvature radius,  $w$  is the width of the channel,  $h$  is the depth of the channel, and  $P$  is the pitch. The channel has a square cross section where  $w$  is equal to  $h$ . Cartesian coordinate system was used in this study, with the  $x$ -axis in the direction of the primary axial flow, as shown in Fig. 2.

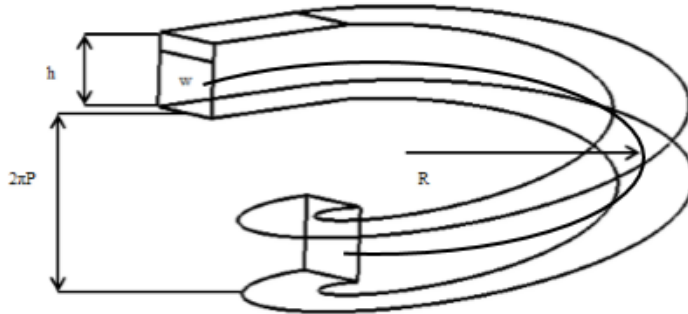


Fig. 1. Helical Channel Physical Model.

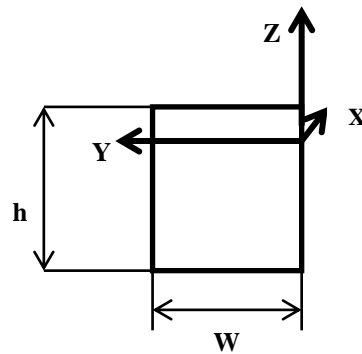


Fig. 2. Cross Section of a Rectangular Channel Showing the Coordinate System.

The analyses in this study were carried out for helical channels as specified in Tables 1 and 2. The channels were of one turn and with square cross sectional area ( $0.4 \text{ m} \times 0.4 \text{ m}$ ).

Table 1. Helical Channels Main Geometrical Specifications for Group (A) of Fixed Pitch ( $P$ ).

Case	$2\pi P$ (m)	$P$ (m)	$R$ (m)	Torsion ( $\lambda$ )	Curvature ( $\delta$ )
1		0.079	0.375	0.108	0.510
2		0.079	0.500	0.062	0.390
3	0.500	0.079	0.750	0.027	0.263
4		0.079	1.00	0.015	0.198
5		0.079	1.250	0.010	0.159

**Table 2. Helical Channels Main Geometrical Specifications for Group (B) of Fixed Curvature Radius (R).**

Case	2πP (m)	P (m)	R (m)	Torsion (λ)	Curvature (δ)
1	0.500	0.079	1.000	0.015	0.198
2	0.750	0.119		0.023	0.197
3	1.000	0.159		0.031	0.195
4	1.250	0.198		0.038	0.192

### 3. Governing Equations

Incompressible, viscous, unsteady and turbulent water fluid flow was investigated in the helical channels, taking into consideration of the fully developed flow in the channels. The curvature δ and the torsion λ of the helical channels were defined respectively as:

$$\delta = \frac{0.5wR}{P^2 + R^2}, \tag{1}$$

$$\lambda = \frac{0.5wP}{P^2 + R^2} \tag{2}$$

The Reynolds Number (Re) and Froude Number (Fr) for the helical channels can be expressed mathematically as:

$$Re = \frac{\rho U D_h}{\mu}, \tag{3}$$

$$Fr = \frac{U^2}{gh_h} \tag{4}$$

where U is the mean water velocity, D<sub>h</sub> is the hydraulic diameter, h<sub>h</sub> is the hydraulic depth, ρ is the density and μ is the dynamic viscosity. The hydraulic diameter (D<sub>h</sub>) of the helical channels was calculated using:

$$D_h = \frac{4A_C}{P_W} = \frac{2wh_h}{w + h_h} \tag{5}$$

where A<sub>C</sub> is the flow cross sectional area, P<sub>W</sub> is the wetted perimeter.

In any type of helical flows, there is an important non-dimensional physical parameter known as the Dean number DE [8]:

$$DE = Re * \sqrt{\delta} \tag{6}$$

In this study, attention was given to the effects of torsion, curvature, Reynolds, Dean and Froude numbers on the helical channel flow properties, such as velocity, water volume fraction, hydraulic depth and free surface profiles.

The mathematical description of the free surface flow in ANSYS Fluent is based on the homogenous multiphase Eulerian fluid approach. In this approach, both fluids (air and water) share the same velocity fields and other relevant fields such as temperature, turbulence, etc., and they are separated by a distinct resolvable interface. The governing equations for the unsteady, viscous, turbulent flow are the Navier-Stokes equations, which can be written in the following form:

$$\frac{\partial}{\partial t}(\rho) + \frac{\partial}{\partial x_i}(\rho u_i) = 0.0 \quad (7)$$

$$(\rho u_i) + \frac{\partial}{\partial x_i}(\rho u_i u_j) = -\frac{\partial p}{\partial x_i} + \frac{\partial}{\partial x_i}(-\rho \overline{u'_i u'_j}) + \quad (8)$$

$$\frac{\partial}{\partial x_j} \left[ \mu \left( \frac{\partial u_i}{\partial x_j} + \frac{\partial u_j}{\partial x_i} - \frac{2}{3} \delta_{ij} \frac{\partial u_l}{\partial x_l} \right) \right]$$

where

$$-\rho \overline{u'_i u'_j} = \mu_t \left( \frac{\partial u_i}{\partial x_j} + \frac{\partial u_j}{\partial x_i} \right) - \frac{2}{3} \left( pk + \frac{\partial u_i}{\partial x_i} \right) \delta_{ij} \quad (9)$$

and

$$\rho = \sum_{\alpha=1}^2 r_{\alpha} \rho_{\alpha}, \quad \mu = \sum_{\alpha=1}^2 r_{\alpha} \mu_{\alpha}, \quad \sum_{\alpha=1}^2 r_{\alpha} = 1 \quad (10)$$

The SST turbulent model can be expressed in the following mathematical form:

$$\frac{\partial(pk)}{\partial t} + \frac{\partial}{\partial x_i}(pk u_i) = \frac{\partial}{\partial x_j} \left( \Gamma_k \frac{\partial k}{\partial x_j} \right) + G_k - Y_k \quad (11)$$

$$\frac{\partial(p\omega)}{\partial t} + \frac{\partial}{\partial x_i}(p\omega u_i) = \frac{\partial}{\partial x_j} \left( \Gamma_{\omega} \frac{\partial \omega}{\partial x_j} \right) + G_{\omega} - Y_{\omega} + D_{\omega} \quad (12)$$

In the previous two equations,  $\Gamma_k$  and  $\Gamma_{\omega}$  represent the effective diffusivity for  $k$  and  $\omega$ .  $G_k$  represents the generation of turbulence kinetic energy due to mean velocity gradients, and  $G_{\omega}$  represents the generation of  $\omega$ .  $Y_k$  and  $Y_{\omega}$  represent the dissipation of  $k$  and  $\omega$  due to turbulence.  $D_{\omega}$  represents the cross-diffusion term.

#### 4. Numerical Method

In present study finite volume method [26] was used for discretizing the governing equations in Fluent of ANSYS workbench 10.1 UTM licensed. The convective terms were discretised using Second Order Upwind scheme, and the pressure was interpolated using linear interpolation scheme, while the central difference scheme was utilized for diffusion terms. For the pressure-velocity coupling, the SIMPLE (Semi-Implicit Methods for Pressure-Linked Equation) was utilized. Convergence was monitored through making dimensionless residual sum for all variables across the computational points. The minimum residual sum for convergence was set to  $1 \times 10^{-6}$ . The inlet boundary condition was set with constant mean velocity normal to the inlet. The inlet velocity and water depth at the inlet boundary of the different helical channels in this study were 0.4 m/s and 0.3 m, respectively. The outlet boundary condition was specified by the outflow.

The working fluid was water with the density of 1000 kg/m<sup>3</sup> and kinematic viscosity of  $1 \times 10^{-6}$  m<sup>2</sup>/s, the reference pressure was 1 bar. The walls were set as a no slip condition.

The grid generator of the RANSE code (ICEM CFD) was used for building the required unstructured tetrahedral meshes for the code solver. The computational domain of the channels was meshed with structured tetrahedral mesh elements of the same sizes for the all cases. Several computational grids were tested in this study to check the solution sensitivity, and ultimately the mesh chose the contained unstructured tetrahedral elements that had been used for every case in this study, as given in Table 3.

**Table 3. Numbers of Total Mesh Elements that had been used in Each Case in this Study.**

Case	Number of Mesh Elements	Global Mesh Size (m)
1A	506686	0.025
2A	626780	0.025
3A	870347	0.025
4A, 1B	1102336	0.025
5A	1336134	0.025
2B	1102932	0.025
3B	11111036	0.025
4B	1119916	0.025

## 5. Results and Discussions

The flow in helical channel was found dependent on the effects of centrifugal, pressure and viscous forces. The curvature of the helical channel created centrifugal forces and radial pressure gradient, which led to the generation of secondary flow [27]. The free surface interface position was numerically determined for helical channels, as described in Tables 1 and 2. Figures 3 and 4 illustrate the effect of curvature and torsion on free surface position interface for two groups. It was noticed that the free surface interface was creeping at the outer wall due to the centrifugal and gravitational forces. Also, the free surface position interface at the outer band increased with the increment of curvature and decrease in torsion, thus, cases (1A) and (4B) recorded the maximum free surface interface position at the outer wall in group A and group B, respectively.

The importance of free surface here was that it would determine the area occupied by the water, and could be used as directly to measure the mass flow rate of water. The hydraulic depth, hydraulic diameter ( $D_h$ ) and volume of fluid (VOF), to be defined as the ratio between the flow cross sectional area ( $A_f$ ) and the channel cross section area ( $w \times h$ ) could be calculated by knowing the free surface position interface; refer to Tables 4 and 5 which display the main flow characteristics in the helical channels for group (A) and (B). The flow properties for all cases in the helical channels were observed increased along with higher water mass flow rate. VOF was the most important factor which determined the water quantity in the helical channels; therefore, the mass flow rate of water increased with the increase in VOF and water mean velocity of the channels.

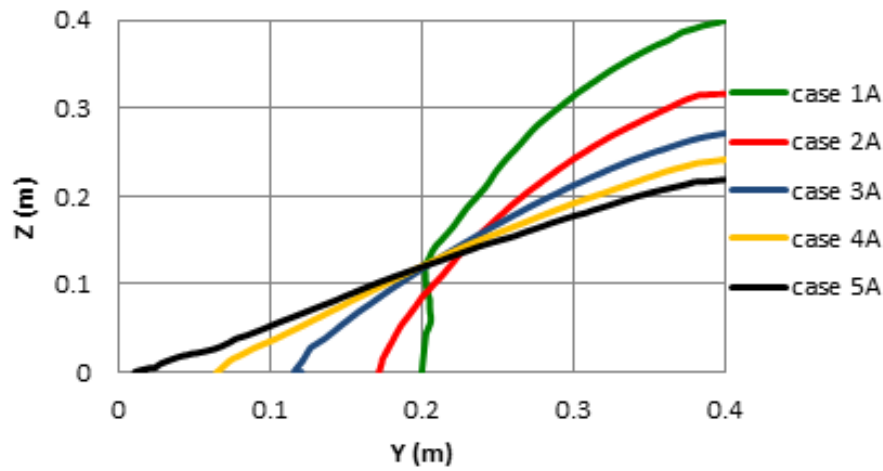


**Fig. 3. Cross Sectional Free Surface Positions Variations at Different Curvature for Group A of Constant Pitch.**

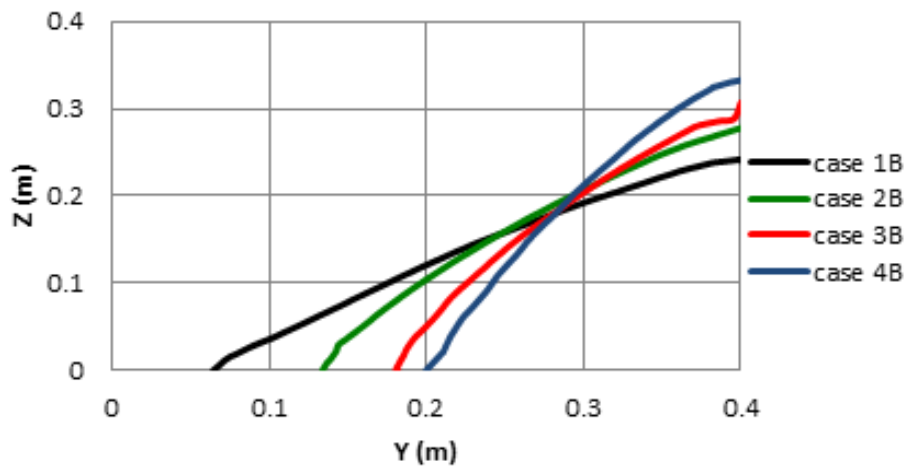


**Fig. 4. Cross Sectional Free Surface Positions Variations with Different Torsion for Group B of Constant Curvature Radius.**

**Table 4. Helical Channels Flow Characteristics for Group (A) in Case of Constant Pitch (P).**

Case	VOF	$U$ (m/s)	Mass flow(kg/s)	$D_h$ (m)	Re $\times 10^5$	DE $\times 10^5$	Fr.
1A	0.245	2.000	78.000	0.157	3.150	2.250	2.020
2A	0.225	2.140	77.200	0.147	3.144	1.960	2.250
3A	0.237	2.148	81.600	0.153	3.290	1.690	2.206
4A	0.250	2.210	88.400	0.160	3.536	1.576	2.210
5A	0.262	2.300	96.600	0.166	3.820	1.525	2.246

**Table 5. Helical Channels Flow Characteristics for Group (B) in Case of Constant Curvature Radius (R).**

Case	VOF	U (m/s)	Mass flow (kg/s)	$D_h$ (m)	Re $\times 10^5$	DE $\times 10^5$	Fr.
1B	0.250	2.210	88.400	0.160	3.780	1.576	2.210
2B	0.230	2.530	93.100	0.149	3.915	1.680	2.630
3B	0.210	2.820	94.200	0.138	4.297	1.730	3.070
4B	0.208	3.120	103.900	0.137	3.784	1.885	3.420

The mean flow velocity inside the helical channel was found decreased with the increase of the curvature, as shown in Fig. 5. The channels flow acquired higher velocity when R increased. In contrast, the flow velocity increased significantly with higher torsion, as indicated in Fig. 6, due to the effect of gravity, which was induced by the channel head.

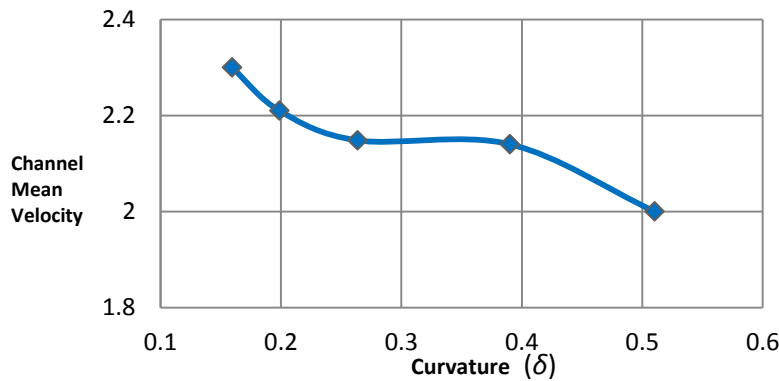


**Fig. 5. Variations of Helical Channel Average Flow Velocity with Curvature ( $\delta$ ) for Group A.**

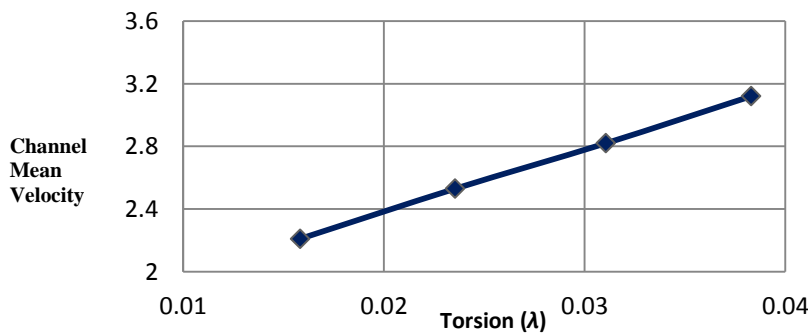


**Fig. 6. Helical Channel Average Velocity Variations with Torsion ( $\lambda$ ) for Group B.**

In general, the Reynolds number dependent not only on the velocity but also on the hydraulic diameter ( $D_h$ ); hence Reynolds number increased with the increment of torsion and the decreasing of curvature, as shown in Figs. 7 and 8. DE was used

to measure the centrifugal force [6, 10] which was induced by curvature. Thus, the DE increased with higher curvature, as shown in Fig. 7. With regard to that, the centrifugal force was reduced when the curvature radius ( $R$ ) was increased. In addition, it showed a little bit of increase with the raise of torsion, as referred to Fig. 8. In other words, the centrifugal force was influenced by the variations of torsion and curvature but it had a lower effect with torsion than curvature.

Froude number ( $Fr$ ) is an important parameter for open channel flow, especially for turbulent flow. When  $Fr > 1$ , the flows are called supercritical flows [28]. It measures the effect of upstream flow on the downstream; this is useful in the case of energy extraction from the channel. Froude number ( $Fr$ ) was observed dependent on mainly stream channel velocity and the hydraulic depth. The effects of torsion and curvature on the Froude Number ( $Fr$ ) are shown in Figs. 7 and 8. It is seen from Figs. 7 and 8 that Froude number ( $Fr$ ) slightly changed with the variation of curvature, while it increased along with the torsion, because the rate of increasing velocities in the case of constant curvature radius was larger than the case of constant pitch, as indicated in Figs. 5 and 6.

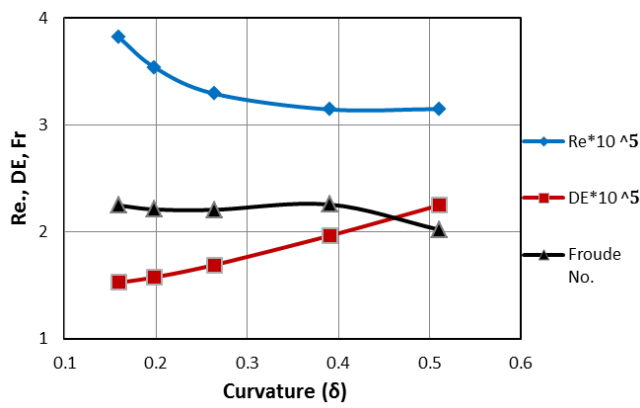


**Fig. 7. Relation between Curvature, Dean, Reynolds and Froude Numbers for Group A of Constant Pitch.**

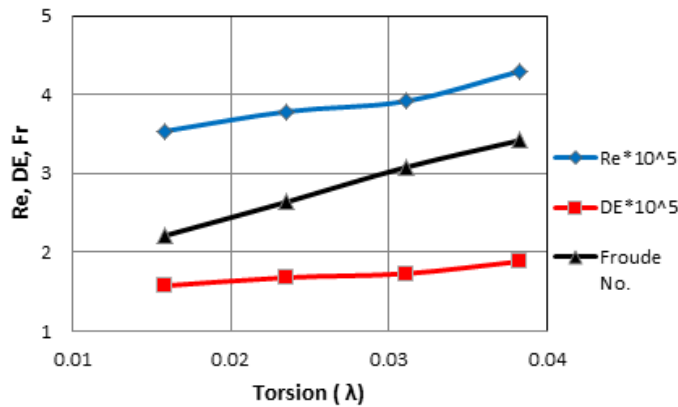


**Fig. 8. Relation between Torsion, Dean, Reynolds and Froude Numbers for Group B of Constant Curvature Radius.**

Figures 9 and 10 display the velocity contours with various physical parameters, including curvature, torsion, Re, DE and Fr. The flow velocities shifted outwardly with the maximum flow velocity near the outside wall of the helical channel due to the effect of centrifugal forces. The flow pattern was diminished, where the curvature of the helical channel became larger and the torsion became lower. On the other hand, the significant values of the velocity were observed at the lower DE for constant pitch, while it increased with DE in the case of increasing torsion.

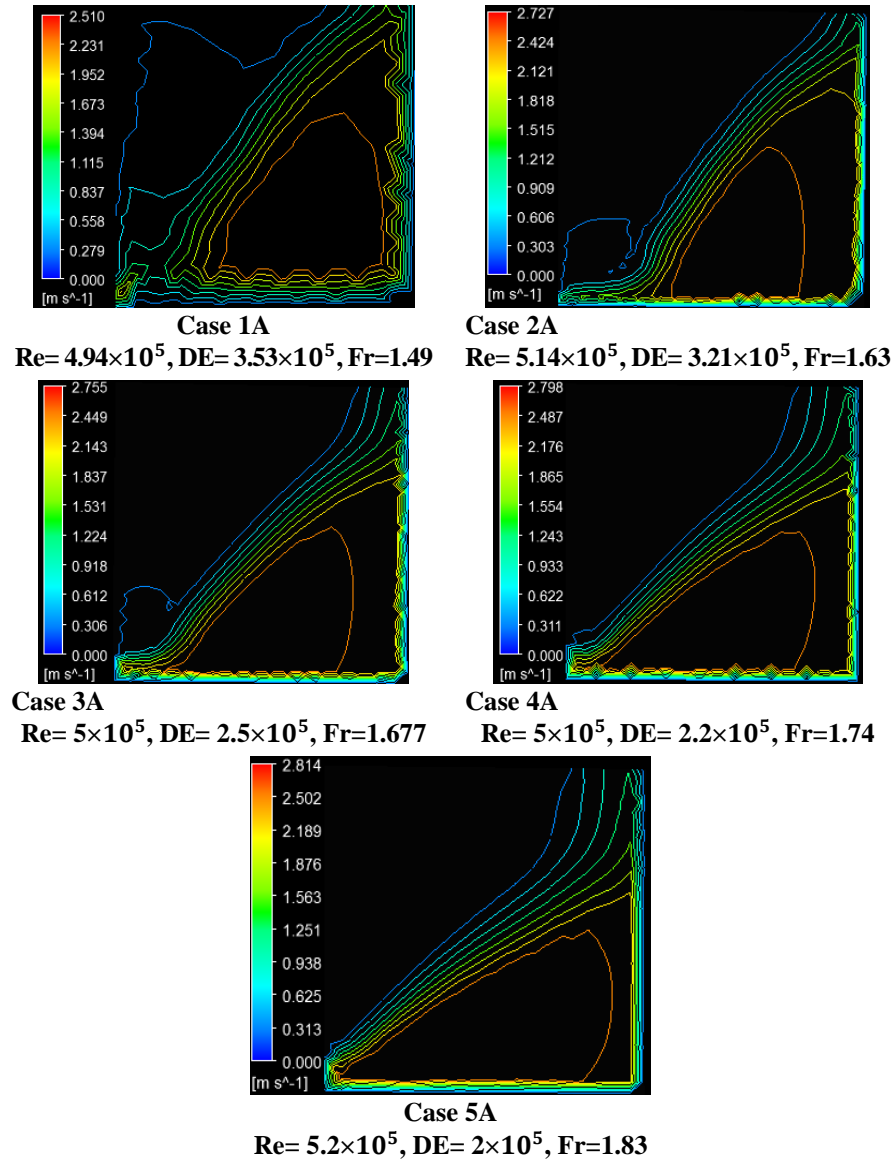


**Fig. 9. Velocity Contours in Plane ( $x=1$  m from the inlet) Normal to Main Flow at Different Curvature for Group A of Constant Pitch.**

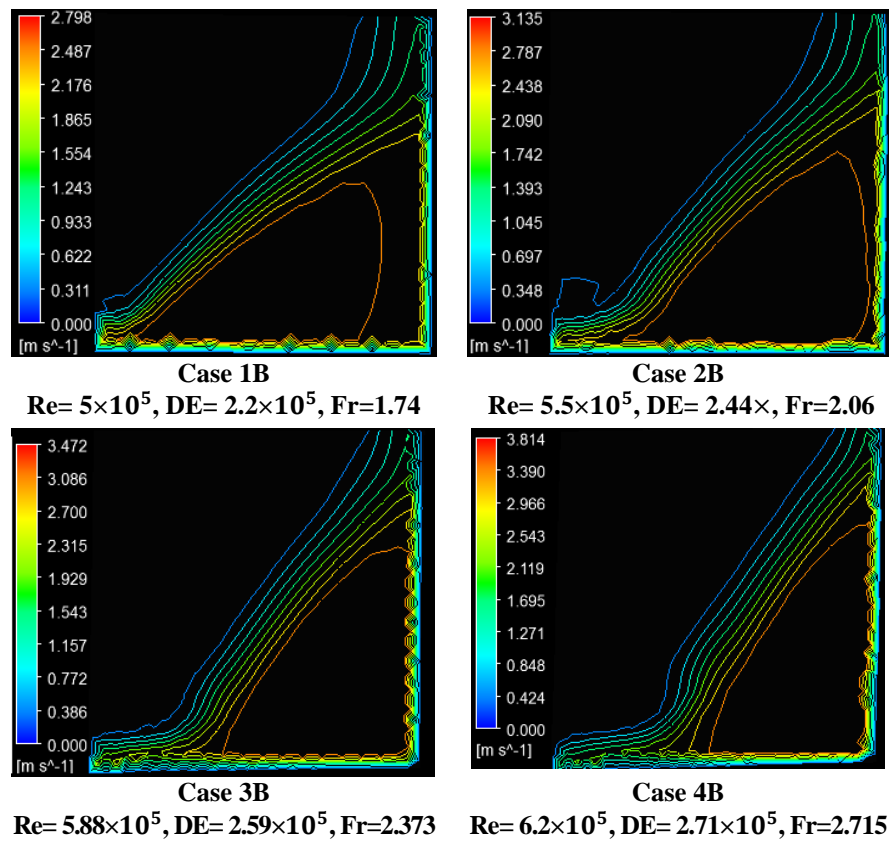


**Fig. 10. Velocity Contours in Plane ( $x=1$  m from the inlet) Normal to Main Flow at Different Torsion for Group B of Constant Curvature Radius.**

## 6. Conclusion

The incompressible viscous water flow inside a helical open flow channels were analyzed using computational fluid dynamics CFD method in this study. The investigation included the effect of torsion, curvature,  $Re$ ,  $Fr$ , and  $DE$  on some hydraulic parameters, such as mean flow velocity of the helical channels, the flow pattern, water region quantity, hydraulic depth and free surface regimes. Flow in helical channel was found dependent on the effects of centrifugal, pressure and viscous forces. Meanwhile, the centrifugal force increased with the increase of the pitch and the decrease in curvature radius. The mean flow velocity shifted towards the outer wall; the flow velocity values would be better with higher torsion and lower curvature. The flow rate of water increased with low values of curvature and high torsion. Moreover, the increase of flow rate improved the properties of helical channels flow. The free surface interface was affected by torsion and curvature changes, which rose at the outer wall when the torsion and curvature grew up at large for given  $DE$ .

## Acknowledgment

The authors would like to express our sincere gratitude to Universiti Teknologi Malaysia (UTM) who assist and provide in the data compilation for this publication.

## References

1. Das, S.K. (1993). Water flow through helical coils in turbulent condition. *The Canadian Journal of Chemical Engineering*, 71(6), 971-973.
2. Williams, G.S.; Clarence, W.H., and George, H.F. (1902). Experiments at Detroit, Michigan, on the effect of curvature upon the flow of water in pipes. *Transactions of the American Society of Civil Engineers*, 47(1), 1-196.
3. Thomson, J. (1876). On the origin of windings of rivers in alluvial plains, with remarks on the flow of water round bends in pipes. *Proceedings of the Royal Society of London*, 25(171-178), 5-8.
4. Thomson, J. (1877). On the origin of windings of rivers in alluvial plains, with remarks on the flow of water round bends in pipes. *Proceedings of the Royal Society of London*, 26(3), 56-57.
5. Eustice, J. (1910). Flow of water in curved pipes. *Proceedings of the Royal Society of London, Series A*, 84(568), 107-118.
6. Dean, W.R. (1927). XVI. Note on the motion of fluid in a curved pipe. *The London, Edinburgh, and Dublin Philosophical Magazine and Journal of Science*, 4(20), 208-223.
7. Dean, W.R. (1928). Fluid motion in a curved channel. *Proceedings of the Royal Society of London, Series A*, 121(787), 402-420.
8. Germano, M. (1982). On the effect of torsion on a helical pipe flow. *Journal of Fluid Mechanics*, 125(1982), 1-8.
9. Germano, M. (1989). The Dean equations extended to a helical pipe flow. *Journal of Fluid Mechanics*, 203(1989), 289-305.
10. Berger, S.A.; and Talbot, L. (1983). Flow in curved pipes. *Annual Review of Fluid Mechanics*, 15, 461-512.
11. Nobari, M.R.H.; and Malvandi, A. (2013). Torsion and curvature effects on fluid flow in a helical annulus. *International Journal of Non-Linear Mechanics*, 57, 90-101
12. Matthews, B.W.; Fletcher, C.A.J.; Partridge, A.C.; and Jancar, A. (1996). *Computational Simulation of Spiral Concentrator Flows in the Mineral Processing Industry*. Chemeca '96.
13. Matthews, B.W.; Fletcher, C.A.J.; and Partridge, A.C. (1997), Computational simulation of fluid and dilute particulate flows on spiral concentrators. *International Conference on CFD in Mineral & Metal Processing and Power Generation*, 101-109.
14. Stokes, Y.M. (2001). Flow in spiral channels of small curvature and torsion. *IUTAM Symposium on Free Surface Flows*, 289-296.
15. Stokes, Y.M. (2001). Computing flow in a spiral particle separator. *Proceedings of 14th Australasian Fluid Mechanics Conference*, Adelaide University, Adelaide, Australia.

16. Schönfeld, F.; and Hardt, S. (2004). Simulation of helical flows in micro channels. *Journal of American Institute of Chemical Engineers*, 50(4), 771-778.
17. Jiang, F.; Drese, K.S.; Hardt, S.; Küpper, M.; and Schönfeld, F. (2004), Helical flows and chaotic mixing in curved micro channels. *American Journal of American Institute of Chemical Engineers*, 50(9), 2297-2305.
18. Fatemeh, G.; and Mahmood, T.H.M. (2013). CFD Simulation of nanosulfur crystallization incorporating population balance modeling. *Iranica Journal of Energy & Environment Special Issue on Nanotechnology*, 4(1), 36-42.
19. Kai-Yo, H.; Chih-Yang, W.; and Yi-Tun, H. (2014). Fluid mixing in a microchannel with longitudinal vortex generators. *Chemical Engineering Journal*, 235(1), 27-36.
20. Peerhossaini, H.; and Le Guer, Y. (1992). Effect of curvature plane orientation on vortex distortion in curved channel flow. *Ordered and Turbulent Patterns in Taylor-Couette Flow*, Springer US, 263-272.
21. Poskas, P.; Simonis, V.; and Ragaisis, V. (2011). Heat transfer in helical channels with two-sided heating in gas flow. *International Journal of Heat and Mass Transfer*, 54(4), 847-853.
22. Simonis, V.; Poskas, P.; and Ragaisis, V. (2012) Enhancement of heat transfer and hydraulic drag in gas-cooled helical channels with artificial roughness on convex wall. *Nuclear Engineering and Design*, 245, 153-160.
23. Morales, R.E.M.; and Eugênio, S.R. (2007). Modeling of free surface flow in a helical channel with finite pitch. *Journal of the Brazilian Society of Mechanical Sciences and Engineering*, 29(4), 345-353.
24. Morales, R.E.M.; and Eugênio, S.R. (2012) Modeling fully developed laminar flow in a helical duct with rectangular cross section and finite pitch. *Applied Mathematical Modelling*, 36(10), 5059-5067.
25. Kim, J.; Parviz, M.; and Robert, M. (1987). Turbulence statistics in fully developed channel flow at low Reynolds number. *Journal of Fluid Mechanics*, 177(1), 133-166.
26. Patankar, S.V. (1980). *Numerical heat transfer and fluid flow*. Taylor & Francis.
27. Nobari, M.R.H.; and Malvandi, A. (2013). Torsion and curvature effects on fluid flow in a helical annulus. *International Journal of Non-Linear Mechanics*, 57, 90-101.
28. Kothandaraman, C.P.; and Rudramoorthy, R. (2007). *Fluid Mechanics and Machinery*. (2<sup>nd</sup> Edition). New Age International Publishers, , 383-393.